Solvent-Responsive Structural Colored Balloons

Kenji Higashiguchi,* Masafumi Inoue, Tomohiro Oda, and Kenji Matsuda*

Department of Synthetic Chemistry and Biological Chemistry, Graduate School of Engineering, Kyoto

University, Katsura, Nishikyo-ku, Kyoto 615-8510, Japan

E-mail: kmatsuda@sbchem.kyoto-u.ac.jp

Polymers.

PS with Low-molecular-weight
$Mn = 1.49 \times 10^4$
$Mw = 4.33 \times 10^4$
$Mw/Mn = 2.90$

PS with High-molecular-weight
$Mn = 2.23 \times 10^5$
$Mw = 4.89 \times 10^5$
$Mw/Mn = 2.19$

Mixture (Low:High = 9:1)
$Mn = 4.04 \times 10^4$
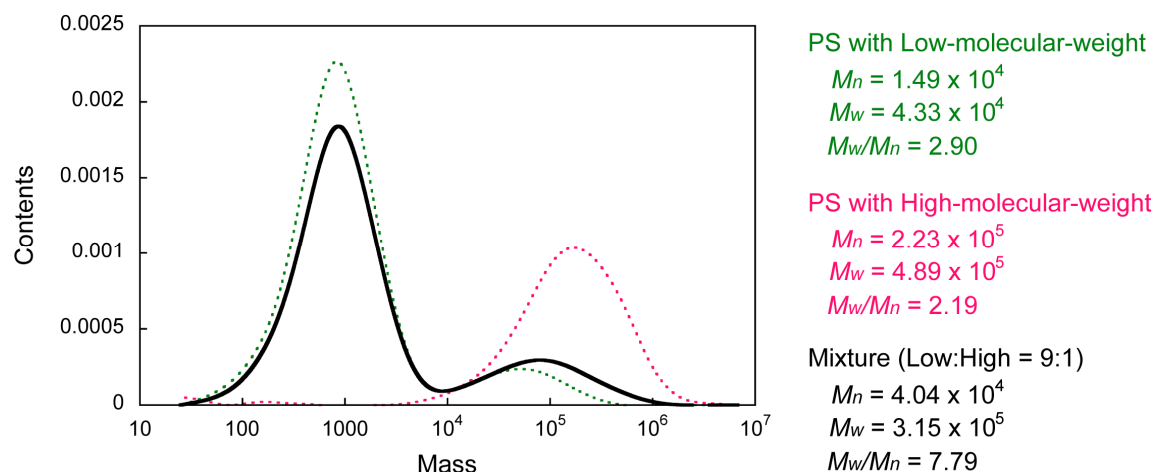$Mw = 3.15 \times 10^5$
$Mw/Mn = 7.79$

Figure S1. GPC chromatogram of PS. Low-molecular weight PS (green dotted line), high-molecular weight PS (red dotted line) and the mixture with the 9:1 ratio of PS with low- and high-molecular weight (black solid line). T_g of the PS mixture was 66°C.
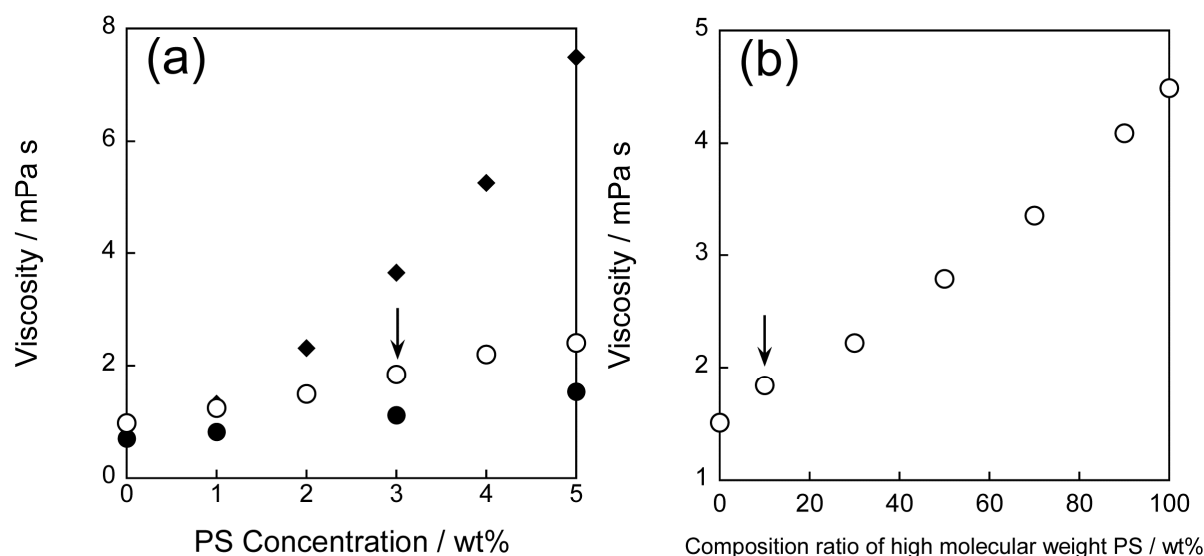

Figure S2. Viscosity of PS solution in dichloromethane. The marked plots by arrows mean the mainly-used solution for preparation of SCBs; the ratio of low- to high-molecular weight was 9:1 and the concentration was 3 wt%. (a) Relationship between viscosity and concentration of PS solution; high molecular weight (closed rhombus), low molecular weight (closed circle), and the polymer mixture (the ratio of low- to high-molecular weight was 9:1) (open circle). (b) Relationship between viscosity and the ratio of PS mixture in dichloromethane. The concentration of the solution was 3 wt%.
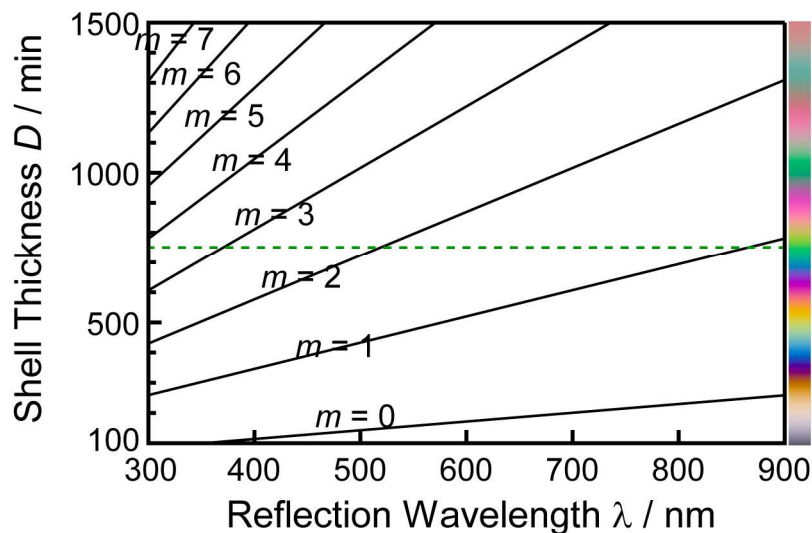
2

Multiple Interference.

Figure S3. Relationship between the shell thickness and reflection wavelength described in the literature[9]. Calculated interference color considering multiple interference was also shown at right axis. The solid lines correspond to the wavelength satisfying the condition for constructive interference at several orders as described by the equation (1). Green dotted line means the balloon shown in Figure 3 ($D = 750$ nm). The intersections to black solid lines show the reflection maxima, however only one wavelength was in visible range at 518 nm ($m = 2$).
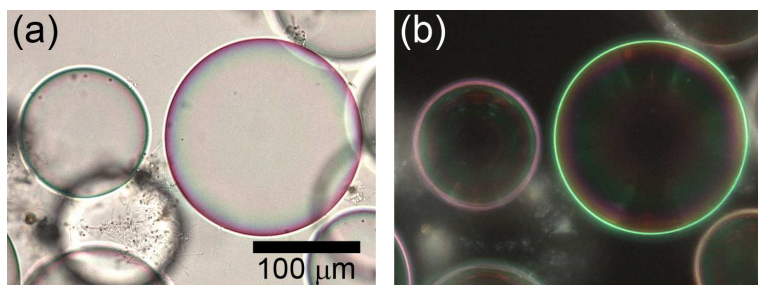
Dependence on the Angle of Incident Light.

Figure S4. Optical microscope images of the SCBs under (a) bright-field and (b) dark-field illumination.

Solvent Exchange.

The exchange of surrounding solvents of SCB was carried out as follows. Acetone and water were mixed in advance by the appropriate ratio. To measure the developing color of SCB, an SCB was picked up from a vial with surrounding water by fine pipette and added into a flow-cell. The solvent mixture was introduced slowly by a syringe pump (Figure S3) and SCBs were observed by an optical microscope. The exchange started at 6 min and almost finished after 10 min as shown in Figure S4. Thus, this *10 min* was defined as "*0 min*" in the text.
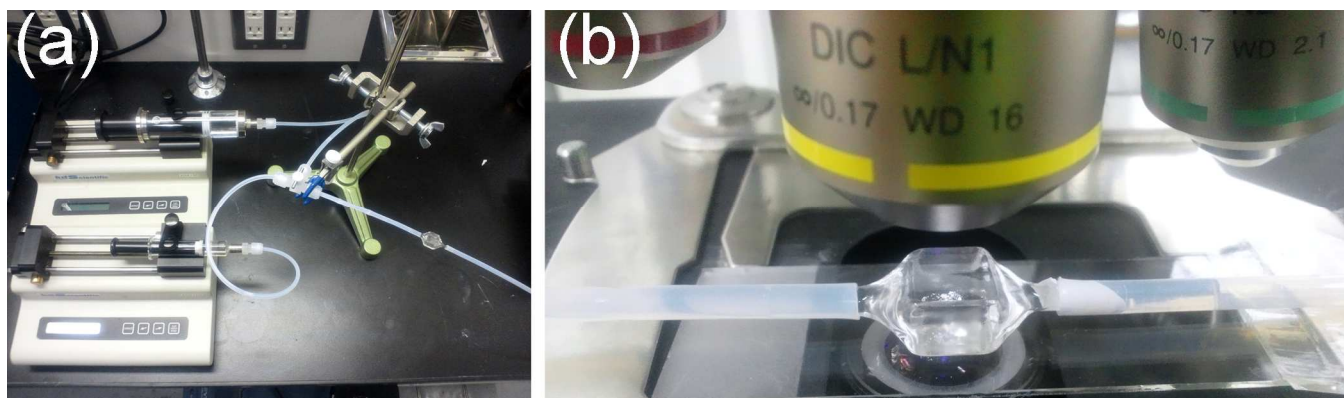

Figure S5. (a) Apparatus used for the exchange of the solvent surrounding SCB. (b) Light path of the flow cell is 5 mm.
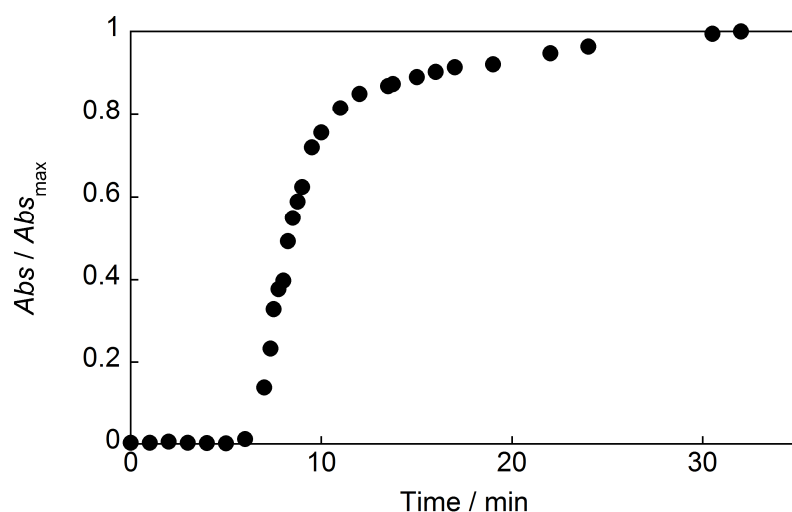

Figure S6. Time-course of the exchange ratio of the internal solvent from water to acetone/water = 4/6, that was labeled by Rhodamine B. The flow rate is set as 0.17 mL/min.

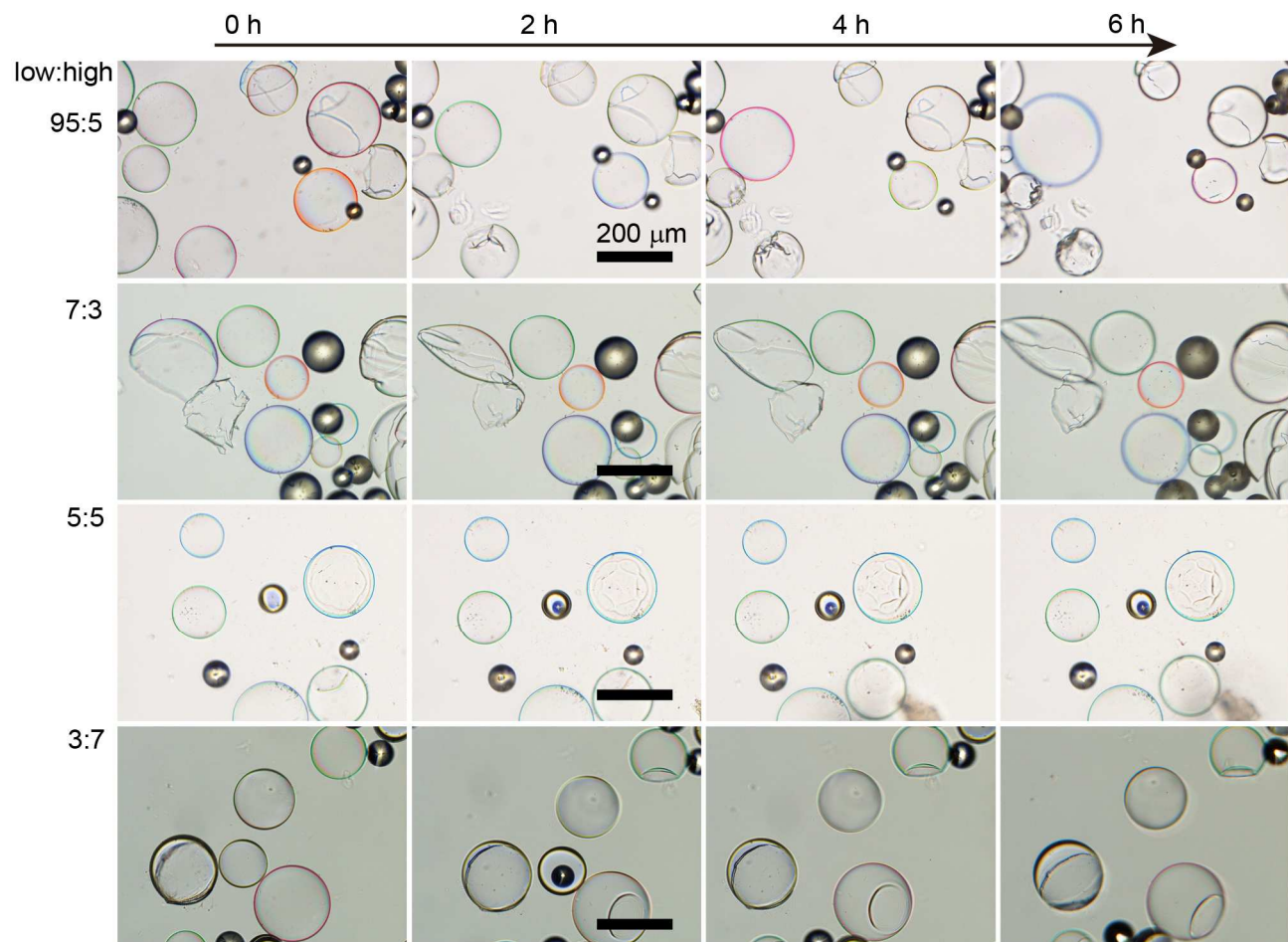**Responsiveness to the Solvent Surrounding SCBs.**

Figure S7. Optical microscope images of the SCBs using mixture of low-and high-molecular weight with several ratio under acetone/water = 4/6. In the case of the mixture with the ratio of low- to high-molecular weight PS being 95:5 and 9:1, the SCBs had high responsiveness to the solvent.
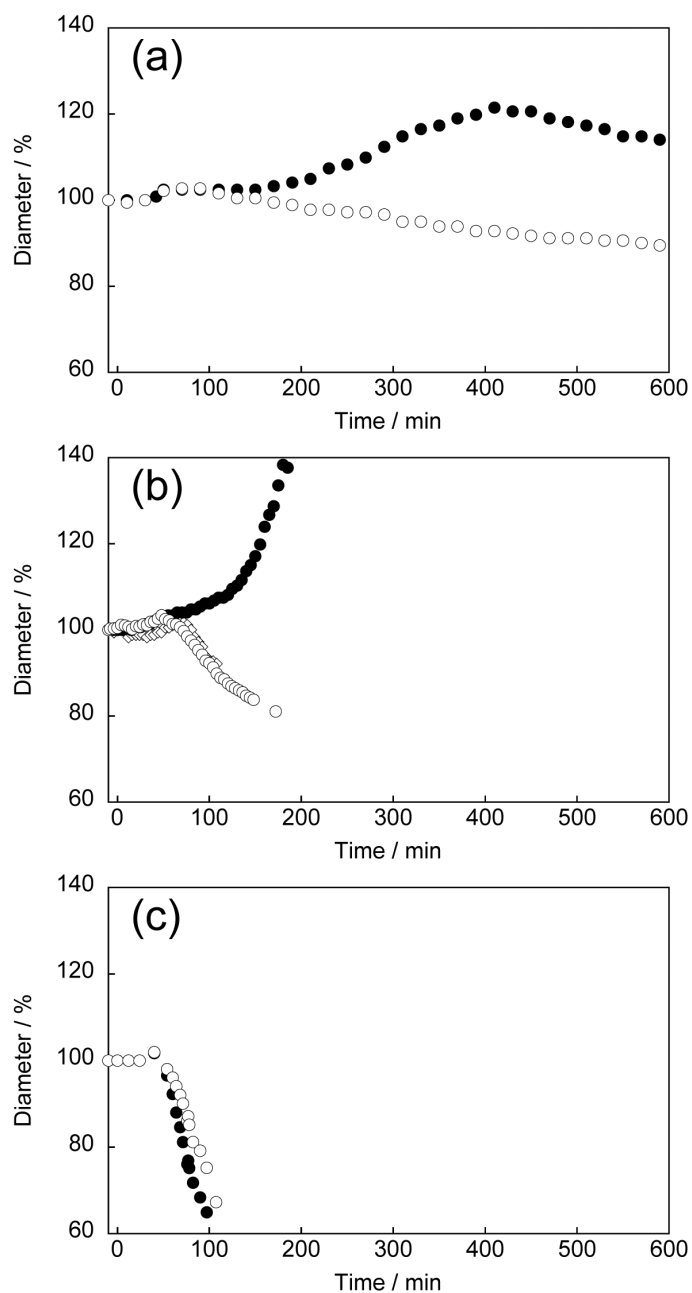
Figure S8. Time course of the diameter change of some SCBs in the ratio of acetone/water mixture of (a) 3:7, (b) 4:6, and (c) 5:5. The change of diameter was shown by the ratio because of the large size distribution of SCBs. The SCBs represented as filled and open circles of (b) were described in the section of Swelling and Shrinking, respectively. In another case, SCBs selected randomly were plotted using some symbols.
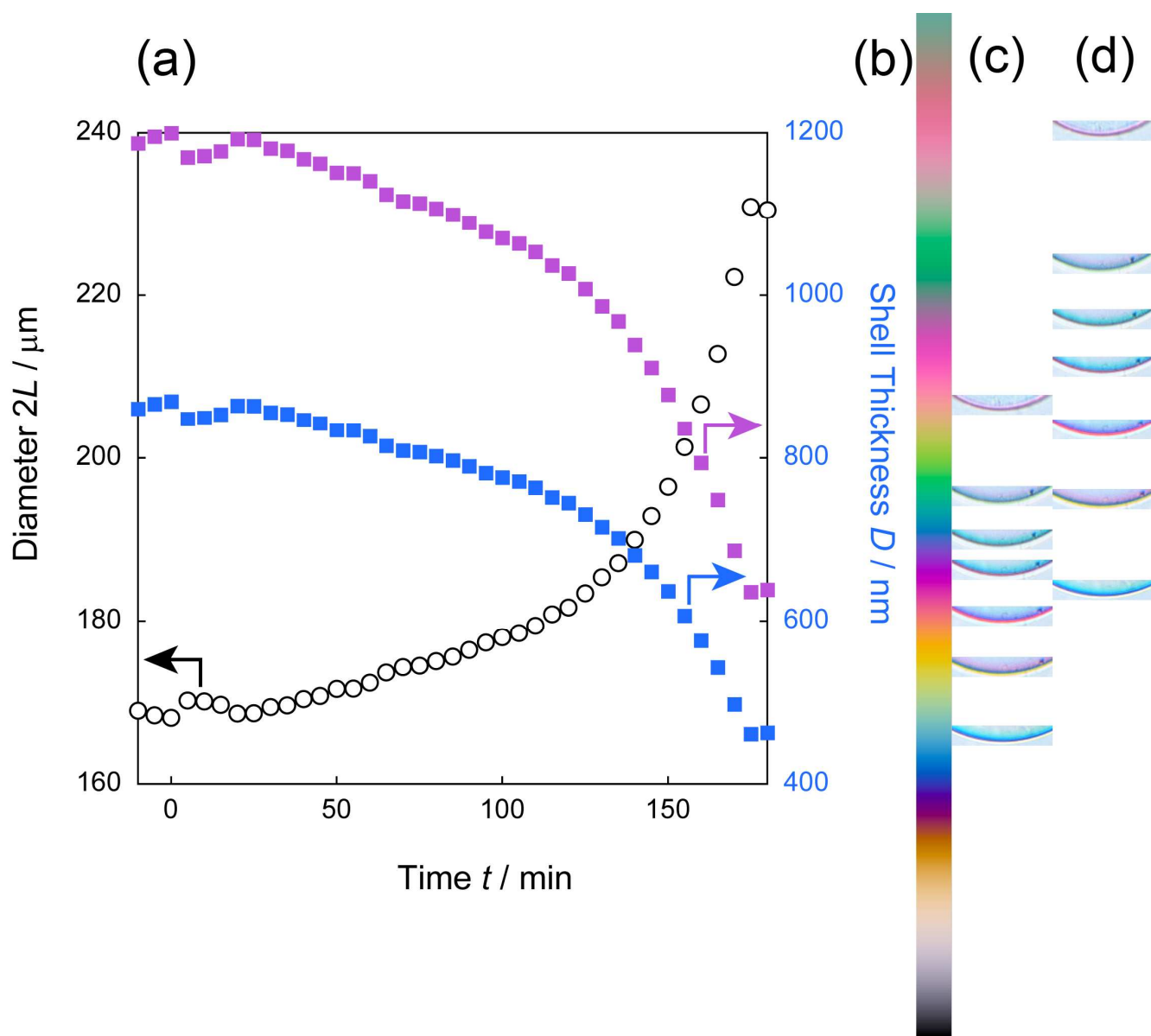
Initial Shell Thickness.

Figure S9. (a) Changes in diameter (open circles) and the expected shell thickness. The shell thicknesses were calculated using $D_0 = 870$ nm (blue solid square) and 1200 nm (purple solid square). (b) Calculated interference color considering multiple interference. The magnified image of SCBs, the y-axis was aligned by the expected shell thickness using (c) $D_0 = 870$ nm and (d) 1200 nm.

Shrinking of Shard.

PS shard showed folding by exposure acetone/water mixture, which was not observed in water. The reason is that the solvated PS given elastic property should deform to decrease the surface energy. Thus, the balloons exposed to acetone/water shrink until the size below the initial state. However, because of the lack of cusp, balloons could not fold and the shell thickness became thick.
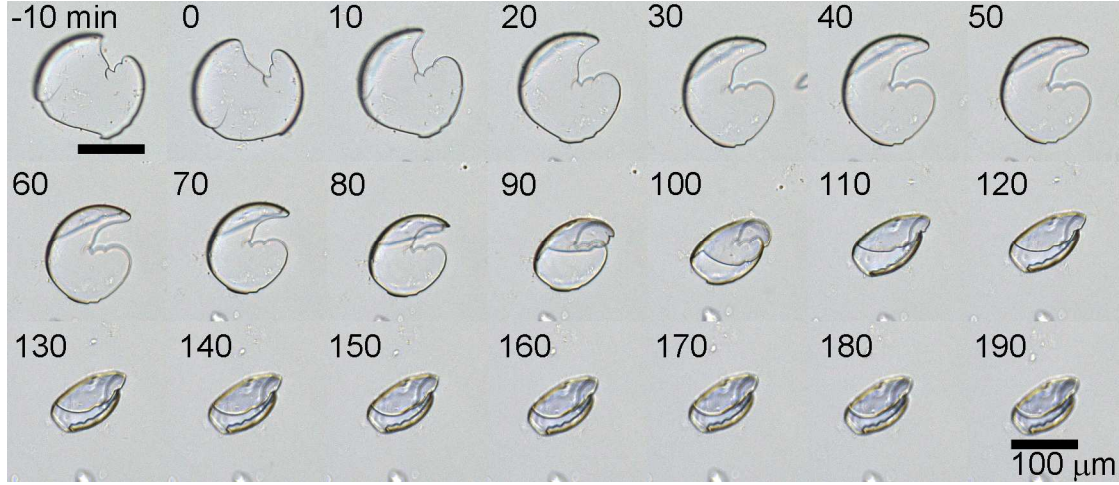

Figure S10. Optical microscope images of a shard using mixture of low- to high-molecular weight PS being 9:1 under acetone/water = 4/6. The folding mainly occurred after 60 min similar to the cases of swelling and shrinking because these deformations require the softening by solvation of PS.

Diffusion coefficient of PS film.

The radius of the balloon L is described as in eq. (5).

$$\frac{1}{2}L^2 = A\int \delta(t)\mathrm{d}t + a_1 \qquad (5)$$

The diffusion coefficient $\delta(t)$ changed with the solvation of the PS film. Here, a linear function is employed for $\delta(t)$ as eq. (S1).

$$\delta_1(t) = \delta_{max}t/t_1 \qquad (0 < t < t_1) \qquad (S1)$$

$$\delta_2(t) = \delta_{max} \qquad (t_1 < t) \qquad (S2)$$

where t_1 represents the boundary between solvating and completely solvated states, therefore, $\delta_1(t_1) = \delta_2(t_1) = \delta_{max}$. Equations (S1) and (S2) are substituted into eq. (5), and the time-dependent changes in the radius are obtained as eq. (S3) and (S4).

$$L_1^{\ 2} = A\frac{\delta_{max}}{t_1}t^2 + B \qquad\qquad (0 < t < t_1) \qquad (S3)$$

$$L_2^{\ 2} = A\delta_{max}(2t - t_1) + B \qquad (t_1 < \ t) \qquad (S4)$$

By least-square fitting, t_1, δ_{max}, A, B were optimized as 224 min, 21.1 μm^2 min^{-1}, 1.5, and 6.85×10^3 μm^2, respectively. The fitted curve shows disagreement (Figure S11).
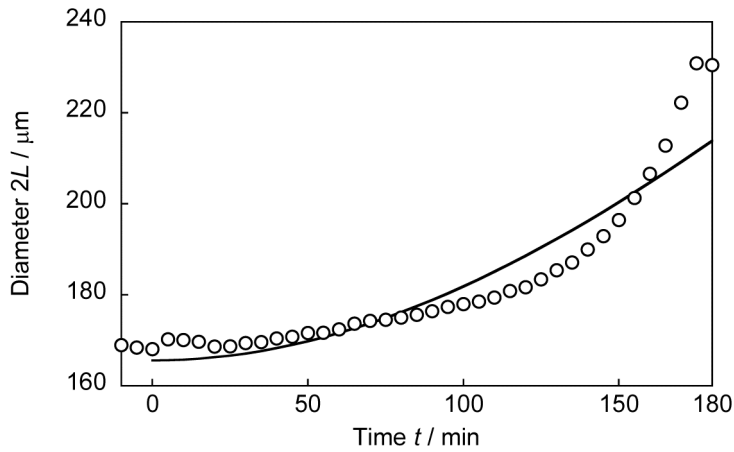

Figure S11. Changes in diameter of the SCB (open circle) with the fitted curve derived from the linear function (solid line). The experimental data is as same as shown in Figure 4.